Inorganic Chemistry

ARTICLE

pubs.acs.org/IC

New Functionalized Flexible Al-MIL-53-X (X = -Cl, -Br, -CH_3, -NO_2, -$(OH)_2$) Solids: Syntheses, Characterization, Sorption, and Breathing Behavior

Shyam Biswas, Tim Ahnfeldt, and Norbert Stock*

Institut für Anorganische Chemie, Christian-Albrechts-Universität, Max-Eyth-Strasse 2, 24118 Kiel, Germany

Supporting Information

ABSTRACT: Five new flexible functionalized aluminum hydroxo terephthalates [Al(OH)(BDC-X)]·*n*(guests) (BDC = 1,4-benzene-dicarboxylate; X = -Cl, **1-Cl**; -Br, **2-Br**; -CH_3, **3-CH_3**; -NO_2, **4-NO_2**; -$(OH)_2$, **5-OH_2**) were synthesized under solvothermal conditions. The as synthesized (Al-MIL-53-X-AS) as well as the activated compounds were characterized by X-ray powder diffraction (XRPD), IR spectroscopy, thermogravimetric (TG), and elemental analysis. Activation, that is, removal of unreacted H_2BDC-X molecules and/or occluded solvent molecules, followed by hydration in air at room temperature, led to the narrow pore (NP) form of the title compounds [Al(OH)(BDC-X)]·*n*(H_2O) (Al-MIL-53-X). Thermogravimetric analysis (TGA) and temperature-dependent XRPD (TDXRPD) experiments performed on the NP-form of the compounds indicate high thermal stability in the range 325−500 °C. As verified by N_2, CO_2, or H_2O sorption measurements, most of the thermally activated compounds exhibit significant microporosity. Similar to pristine Al-MIL-53, the present compounds retain their structural flexibility depending on the nature of guest molecules and temperature, as verified by cell parameter determination from XRPD data. The breathing behavior of the functionalized frameworks upon dehydration−rehydration, investigated by temperature and time-dependent XRPD measurements, differs significantly compared to parent Al-MIL-53.

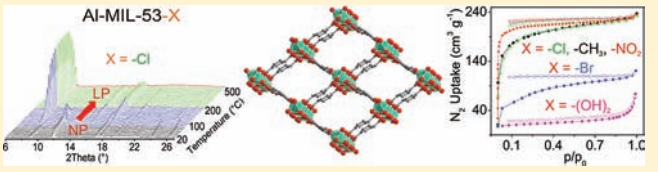

INTRODUCTION

Metal−organic frameworks (MOFs),[1−3] which are constructed of inorganic building units and organic linkers, are attracting considerable interest because of their potential applications in areas such as catalysis,[4,5] gas storage/separation,[6−8] and drug delivery.[9,10]

Because of the modular character of MOFs various pore shapes and functionalities can be achieved by varying the metal as well as the organic linker molecules. A series of compounds based on the MIL-53 topology has been reported, where various trivalent metal ions as well as different ditopic organic linker molecules varying in size and functionality have been incorporated.[11−15] The MIL-53 structure contains chains of *trans* corner-sharing [$MO_4(OH)_2$] polyhedra that are connected to each other by aryldicarboxylate linker molecules, $(O_2C-C_6H_4-CO_2)^{2-}$, and thus one-dimensional channels are formed (Figure 1). The compounds have the general composition [M(OH)($O_2C-C_6H_4-CO_2$)] with M = Cr,[11] Fe,[12] Al,[13] Ga,[14] and In.[15] One outstanding property of these compounds is their reversible framework flexibility, also denoted as breathing,[16] which depends strongly on the incorporated metal ion,[17,18] size and functionality of the linker molecules,[19] the temperature[17,18] as well as the nature of the guest molecules.[11,13,20] Thus many studies have been performed with carbon dioxide,[21−29] linear alkanes,[30−33] or xylenes[34,35] as guest molecules. Depending on these parameters a narrow or a large pore form is observed (Figure 1), and the transformation can lead to a change in unit cell volume up to 40%.[19]

The iron series has been investigated in great depth. Thus, seven functionalized Fe-MIL-53 compounds[19,36,37] have been reported. The effect on the structure flexibility of the dry as well as guest containing forms was evaluated using various characterization methods ranging from X-ray powder diffraction and IR spectroscopy to computational studies. Through the use of chemical groups differing in polarity, hydrophilicity, and acidity, the authors were able to demonstrate that the presence of intraframework interactions dominate the geometry of the pore opening rather than their steric properties.

Al-based MOFs are lightweight, nontoxic, and most of these materials are stable against hydrolysis.[38−40] Compared to the Fe-MIL-53 compounds the number of known functionalized Al-based analogues is smaller and little is know about the temperature dependent structural properties. Thus Al-MIL-53-NH_2,[41−43] Al-MIL-53-OH,[44] Al-MIL-53-$(CO_2H)_2$,[45] and Al-MIL-53-C_4H_4 (Al-PCP)[46] have been reported, and the amino as well as the hydroxyl derivative have been employed for post-synthetic modification reactions.[44−49] The unfunctionalized compound Al-MIL-53 was also used as a host material.[50−52]

Inspired by the advantages of Al-based MOFs, and the interest that the known Al-MIL-53 based compounds have attracted, we have introduced five different functional groups (polar: -Cl, -Br, -NO_2; acidic: -OH; nonpolar: -CH_3) into parent Al-MIL-53 framework to evaluate by X-ray diffraction, IR spectroscopy,

Received: June 7, 2011
Published: September 07, 2011

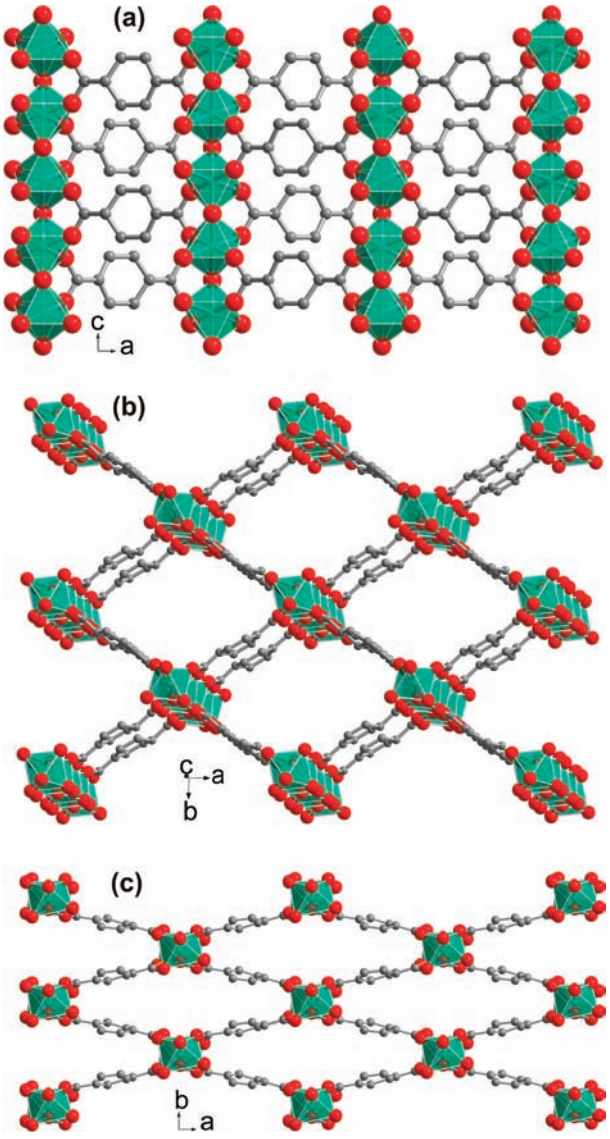

Figure 1. Ball-and-stick representations of the 3D framework structure of Al-MIL-53 with Al atoms displayed as octahedra (color codes: Al, bluish green; C, gray; O, red). (a) Infinite chains of corner-sharing octahedral $[AlO_4(OH)_2]$ units interconnected by the BDC linkers. (b, c) The large pore (LP) and narrow pore (NP) forms of the framework viewed along the crystallographic *c*-axis. For clarity, hydrogen atoms and guest molecules have been omitted from all structural plots. The figure was drawn using structural data taken from ref 13.

TG, and sorption analysis the effect of such organic modifications (Scheme 1) both on the pore surface properties and breathing behavior. In this article, we report on the syntheses, characterization, sorption and breathing properties of the above-mentioned flexible functionalized Al-MIL-53-X solids (X = -Cl, -Br, $-CH_3$, $-NO_2$, $-(OH)_2$).

EXPERIMENTAL SECTION

Materials and General Methods. The H_2BDC-Cl and H_2BDC-CH_3 ligands were synthesized according to previously published procedures.[19] All other starting materials were of reagent grade and used as received from the commercial supplier. Fourier transform infrared (FTIR) spectra were recorded in the range 4000−400 cm^{-1} on an ALPHA-ST-IR Bruker spectrometer with an ATR unit. Elemental analyses (C, H, N) were carried out on a Eurovektor EuroEA Elemental Analyzer. Thermogravimetric analysis (TGA) was performed with a Netzsch STA-409CD thermal analyzer in a temperature range of 25−800 °C under air atmosphere at a heating rate of 4 °C min^{-1}. Ambient temperature X-ray powder diffraction (XRPD) patterns were measured using CuKα radiation (λ = 1.5406 Å) with a STOE STADI P diffractometer equipped with a linear position-sensitive detector (LPSD) or a STOE high-throughput powder diffractometer equipped with an image-plate position-sensitive detector (IPPSD). Lattice parameters were determined using the DICVOL program[53] and refined using STOE's WinXPow[54] software package. Temperature-dependent X-ray powder diffraction (TDXRPD) experiments were performed under air atmosphere with a STOE STADI P diffractometer equipped with an IPPSD detector and a STOE capillary furnace (version 0.65.1) using CuKα radiation. For **4-NO_2-AS**, each pattern was recorded at intervals of 15 °C. For all the other compounds, the patterns below and above 200 °C were collected at intervals of 10 and 25 °C, respectively. The N_2, CO_2, and H_2O sorption isotherms up to 1 bar were measured using a Belsorp Max apparatus at −196, 25, and 25 °C, respectively. The NP-forms of the compounds were heated (155 °C, 12 h for **1-Cl**, **2-Br**, and **3-CH_3**; 130 °C, 6 h for **4-NO_2** and **5-$(OH)_2$**) under dynamic vacuum prior to sorption experiments.

Caution! *Perchlorate salt is potentially explosive, and caution should be exercised when dealing with such material. However, the small quantities used in this study were not found to present a hazard.*

Elemental analyses and frequencies of infrared bands for all the compounds are presented in Supporting Information, Tables S2 and S3, respectively.

Al-MIL-53[13,33] and Al-MIL-53-NH_2[43] were synthesized and activated according to literature methods. The usual characterization experiments (XRPD, TGA, IR spectroscopy, and sorption analysis) were performed to confirm their purity.

Synthesis of Al-MIL-53-Cl-AS (1-Cl-AS). A mixture of $AlCl_3 \cdot 6H_2O$ (1.0 g, 4.14 mmol), H_2BDC-Cl (0.83 g, 4.14 mmol), and water (40 mL) was placed in a 100 mL Teflon liner, and the resulting mixture was heated in a conventional oven at 210 °C for 12 h and cooled to room temperature. The white product was obtained by filtration. The yield was 0.74 g (2.84 mmol, 69%) based on the Al salt.

Synthesis of Al-MIL-53-Br-AS (2-Br-AS). A mixture of $Al(NO_3)_3 \cdot 9H_2O$ (1.5 g, 3.99 mmol), H_2BDC-Br (0.98 g, 3.99 mmol), benzoic acid (0.25 g, 2.04 mmol) and water (60 mL) was placed in a 100 mL Teflon liner, and the resulting mixture was heated in a conventional oven at 210 °C for 12 h and cooled to room temperature. The white product was collected by filtration. The yield was 0.95 g (2.49 mmol, 63%) based on the Al salt.

Synthesis of Al-MIL-53-CH_3-AS (3-CH_3-AS). A mixture of $AlCl_3 \cdot 6H_2O$ (1.0 g, 4.14 mmol), H_2BDC-CH_3 (0.75 g, 4.16 mmol), and water (40 mL) was placed in a 100 mL Teflon liner, and the resulting mixture was heated in a conventional oven at 210 °C for 12 h and cooled to room temperature. The white product was obtained by filtration. The yield was 0.65 g (1.66 mmol, 40%) based on the Al salt.

Scheme 1. Modified Terephthalic Acid Ligands H_2BDC-X Used for Synthesizing Al-MIL-53-X Materials

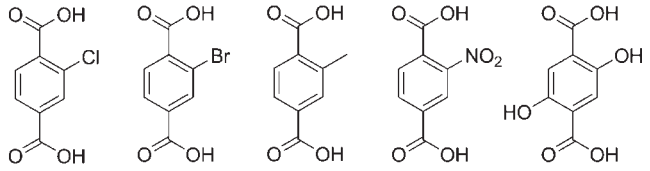

dx.doi.org/10.1021/ic201219g |*Inorg. Chem.* 2011, 50, 9518–9526

Synthesis of Al-MIL-53-NO_2-AS (4-NO_2-AS). A mixture of $Al(NO_3)_3 \cdot 9H_2O$ (1.49 g, 3.97 mmol), $H_2BDC\text{-}NO_2$ (0.92 g, 4.37 mmol) and water (50 mL) was placed in a 100 mL Teflon liner, and the resulting mixture was heated in a conventional oven at 170 °C for 12 h and cooled to room temperature. The white microcrystalline product was obtained by filtration. The yield was 0.52 g (1.92 mmol, 48%) based on the Al salt.

Synthesis of Al-MIL-53-$(OH)_2$-AS (5-OH_2-AS). A mixture of $Al(ClO_4)_3 \cdot 9H_2O$ (0.98 mg, 2.01 mmol), $H_2BDC\text{-}(OH)_2$ (0.40 g, 2.01 mmol) and *N,N′*-diethylformamide (DEF; 5 mL) was placed in a 27 mL Teflon liner, and the resulting mixture was heated in a conventional oven at 125 °C for 5 h and cooled to room temperature. The yellow product was collected by filtration. The yield was 0.78 g (3.02 mmol, 67%) based on the Al salt.

Activation of Al-MIL-53-X-AS Materials. All the AS-materials were activated in two steps.

Each (1.0 g) of **1-Cl-AS**, **2-Br-AS**, and **3-CH_3-AS** was heated in *N,N′*-dimethylformamide (DMF; 60 mL) at 155 °C for 24 h in a conventional oven. The filtered solids (denoted Al-MIL-53-X-DMF) were heated at 155 °C for 24 h in a conventional oven.

Compound **4-NO_2-AS** (0.5 g) was heated in methanol (2 × 60 mL) at 80 °C in a conventional oven for 48 h, during which period the solvent was discarded and fresh solvent was added after 24 h. The filtered white solid was heated at 150 °C for 12 h in a conventional oven.

Compound **5-$(OH)_2$-AS** (0.2 g) was heated in 200 mL of methanol/water (50:50, v/v) at 100 °C in a conventional oven for 12 h. The yellow solid was collected by filtration, washed with water (named **5-$(OH)_2$-H_2O** or water-rich form) and heated at 130 °C for 12 h in a conventional oven.

RESULTS AND DISCUSSION

Syntheses and Activation. The synthesis procedures adopted for the functionalized compounds differ significantly with respect to the one previously reported for pristine Al-MIL-53.[13] To optimize synthesis conditions for the Al-MIL-53-X solids, stoichiometric mixtures (1:1) of aluminum salts (nitrate, chloride, perchlorate, and sulfate) and H_2BDC-X ligands were heated in polar solvents such as H_2O, methanol, DMF, DEF, or DMA (*N,N′*-dimethylacetamide). Water was found as the best solvent for the preparation of all compounds, except **5-$(OH)_2$**. The use of DEF instead of water led to the formation of highly crystalline **5-$(OH)_2$-AS**. Whereas **1-Cl-AS**, **3-CH_3-AS**, and **4-NO_2-AS** can be synthesized with $Al(NO_3)_3 \cdot 9H_2O$ and $AlCl_3 \cdot 6H_2O$, **2-Br-AS** and **5-$(OH)_2$-AS** with high crystallinity were only obtained with $Al(NO_3)_3 \cdot 9H_2O$ and $Al(ClO_4)_3 \cdot 9H_2O$, respectively.

The AS-forms of the compounds contain guest molecules (H_2BDC-X linkers, H_2O or DEF) trapped in the pores which could not be removed by direct thermal treatment (see Thermal Behavior section). They were activated in a two-step procedure similar to that reported for Al-MIL-53[33] and Al-MIL-53-NH_2.[43] At first, the guest molecules were exchanged by heating the AS-compounds with polar solvents such as DMF (**1-Cl-AS**, **2-Br-AS**, and **3-CH_3-AS**), methanol (**4-NO_2-AS**), or a methanol/water (50:50, v/v) mixture (**5-$(OH)_2$-AS**). In a second step, the polar solvent molecules were removed by heating the exchanged solids under air atmosphere. After cooling to room temperature, the activated compounds adsorb different amounts of water (Supporting Information, Table S1) from air depending on the attached functional groups.

Structure Description. The framework topology of all the functionalized compounds is identical, and they correspond to the pristine Al-MIL-53 structure (Figure 1).[13] The 4^4 net of Al-MIL-53 contains infinite tilted *trans* chains (Figure 1a) of corner-sharing (via μ_2-OH group) $[AlO_4(OH)_2]$ octahedra, which are connected through the carboxylate groups of the BDC linkers to form a three-dimensional (3D) framework possessing one-dimensional (1D) rhombic-shaped pores. In the AS-forms of the functionalized solids, the 1D channels are occupied by guest molecules (solvent molecules or H_2BDC-X linkers) at ambient conditions. Depending on both the nature of guest molecules[11,13,20] and the temperature,[17,18] the frameworks reversibly change from a narrow pore (NP; crystal system: monoclinic; unit cell volume: ~1000 Å^3) to a large pore (LP; crystal system: orthorhombic; unit cell volume: ~1400−1500 Å^3) form (Figures 1b,c, Table 1 and Breathing Behavior section) with up to 50% variation of their unit cell volume without breaking any bond and changing the framework topology.

Infrared Spectroscopy. The FT-IR spectra of AS, guest-exchanged and NP-forms of each of the Al-MIL-53-X compounds (Supporting Information, Figures S6−S10 and Tables S3−S4) are very similar, as expected. In the IR spectra of the AS-forms of all the compounds, the strong absorption bands due to asymmetric and symmetric $-CO_2$ stretching vibrations of the coordinated BDC-X linkers are located in the regions 1597−1616 cm^{-1} and 1415−1463 cm^{-1}, respectively.[13] The additional strong absorption bands in the region 1694−1711 cm^{-1}, observed in the IR spectra of AS-forms of **1-Cl**, **2-Br**, **3-CH_3**, and **4-NO_2**, can be attributed to the protonated form ($-CO_2H$) of unreacted or occluded BDC-X ligands.[13] The medium absorption band at 1659 cm^{-1} in the IR spectra of **5-$(OH)_2$-AS** can be assigned to the carbonyl stretching vibration of occluded DEF molecules. The characteristic strong absorption band of the carbonyl stretching vibration of guest DMF molecules appears in the range 1663−1673 cm^{-1} in the IR spectra of DMF-form of all the compounds. The absence of the absorption bands of noncoordinated H_2BDC-X linkers, DMF, and DEF molecules in the IR spectra of NP-form confirms complete activation of the compounds. The C−H stretching vibration of the -CH_3 group attached with the BDC-CH_3 linker exhibits weak absorption bands at about 2970 and 2930 cm^{-1} in the IR spectra of AS, DMF and NP-forms of **3-CH_3**.[55] The characteristic broad absorption band due to stretching vibration of the −OH group appended to BDC-$(OH)_2$ linker is located in the region 3300−3350 cm^{-1} in the IR spectra of AS, guest-exchanged and NP-forms of **5-$(OH)_2$**.[55] The stretching vibration of the μ_2-OH group displays weak absorption band in the region 3630−3680 cm^{-1} in the IR spectra of AS, guest-exchanged and NP-forms of all the compounds.[19]

Thermal Stability. To examine the thermal stability of all Al-MIL-53-X compounds, thermogravimetric analyses (TGA) were performed on both AS and NP-forms of the compounds in air atmosphere. On the basis of the TG analyses, all the compounds are thermally stable up to 325−500 °C. The descending order of thermal stability of the compounds is **1-Cl** (500 °C) > **2-Br** (410 °C) > **4-NO_2** (380 °C) > **3-CH_3** (370 °C) > **5-$(OH)_2$** (325 °C). The highest thermal stability of **1-Cl** equals to that of the nonmodified Al-MIL-53 solid.[13] The lowest thermal stability of **5-$(OH)_2$** can be related to the redox reactivity of the BDC-$(OH)_2$ linker.[56] It is noteworthy that an even lower thermal stability has been reported for Fe-MIL-53-$(OH)_2$ (150−160 °C).[19]

In the TG curves of the AS-forms of all the compounds (Supporting Information, Figures S11−S15), any weight loss step that occurs below the decomposition temperature of the frameworks can be assigned to the removal of the occluded guest molecules (H_2O, H_2BDC-X linkers or DEF). Below the decomposition

Table 1. Molecular Formulae, Refined Lattice Parameters,[a] and Pore Types[b] of the Different Forms of the Al-MIL-53-X Solids

compound	molecular formula	a (Å)	b (Å)	c (Å)	β (deg)	V (Å^3)	pore type
1-Cl-AS	[Al(OH)(BDC-Cl)]·0.85(H_2BDC-Cl)	16.580(7)	13.243(5)	6.666(6)		1453.2(12)	LP
1-Cl-DMF	[Al(OH)(BDC-Cl)]·1.1(DMF)	17.03(4)	12.36(3)	6.616(20)		1392.0(89)	LP
1-Cl	[Al(OH)(BDC-Cl)]·0.5(H_2O)	19.776(4)	7.9371(16)	6.6010(17)	106.589(13)	993.0(5)	NP
1-Cl-HT	[Al(OH)(BDC-Cl)]	16.604(7)	12.985(8)	6.623(4)		1428.1(19)	LP
2-Br-AS	[Al(OH)(BDC-Br)]·0.4(H_2BDC-Br)·0.5(H_2O)	16.532(12)	13.092(14)	6.637(5)		1453.1(25)	LP
2-Br-DMF	[Al(OH)(BDC-Br)]·1.1(DMF)	16.438(15)	13.368(11)	6.653(3)		1462.0(11)	LP
2-Br	[Al(OH)(BDC-Br)]·0.5(H_2O)	19.567(14)	8.532(12)	6.616(5)	107.22(6)	1055.1(23)	NP
1-Br-HT	[Al(OH)(BDC-Br)]	16.372(12)	13.181(11)	6.608(6)		1426.1(26)	LP
3-CH_3-AS	[Al(OH)(BDC-CH_3)]·0.9(H_2BDC-CH_3)·0.2(H_2O)	16.404(5)	13.335(3)	6.649(3)		1456.8(31)	LP
3-CH_3-DMF	[Al(OH)(BDC-CH_3)]·1.1(DMF)	16.93(3)	12.61(4)	6.663(15)		1422.6(86)	LP
3-CH_3	[Al(OH)(BDC-CH_3)]·0.1(H_2O)	19.700(17)	7.999(7)	6.603(5)	106.40(5)	998.1(19)	NP
3-CH_3-HT	[Al(OH)(BDC-CH_3)]	16.545(13)	12.981(14)	6.613(8)		1420.4(30)	LP
4-NO_2-AS	[Al(OH)(BDC-NO_2)]·0.22(H_2BDC-NO_2)·1.4(H_2O)	16.545(6)	13.120(5)	6.670(3)		1447.8(13)	LP
4-NO_2-DMF	[Al(OH)(BDC-NO_2)]·1.0(DMF)	17.367(6)	11.868(5)	6.662(4)		1373.1(8)	LP
4-NO_2	[Al(OH)(BDC-NO_2)]·0.6(H_2O)	19.687(10)	8.257(5)	6.635(3)	106.87(4)	1032.1(12)	NP
4-NO_2-HT	[Al(OH)(BDC-NO_2)]	16.382(7)	13.320(10)	6.6490(17)		1450.8(8)	LP
5-$(OH)_2$-AS	[Al(OH)(BDC-$(OH)_2$)]·0.7(H_2BDC-$(OH)_2$)	17.212(14)	12.284(8)	6.670(7)		1410.4(28)	LP
5-$(OH)_2$-DMF	[Al(OH)(BDC-$(OH)_2$)]·1.0(DMF)	17.62(3)	11.579(8)	6.628(4)		1352.2(34)	LP
5-$(OH)_2$-H_2O	[Al(OH)(BDC-$(OH)_2$)]·5.5(H_2O)	17.397(4)	11.832(4)	6.6284(22)		1364.5(4)	LP
5-$(OH)_2$	[Al(OH)(BDC-$(OH)_2$)]·1.0 (H_2O)	19.762(4)	7.6320(16)	6.5786(14)	105.768(13)	954.9(5)	NP
Al-MIL-53-AS[13]	[Al(OH)(BDC)]·0.7(H_2BDC)	17.129(2)	12.182(1)	6.628(1)		1383.1(2)	LP
Al-MIL-53-DMF	[Al(OH)(BDC)]·1.1(DMF)	17.55(6)	11.396(17)	6.615(13)		1322.8(74)	LP
Al-MIL-53[13]	[Al(OH)(BDC)]·1.0(H_2O)	19.513(2)	7.612(1)	6.576(1)	104.24(1)	946.8(1)	NP
Al-MIL-53-HT[13]	[Al(OH)(BDC)]	16.675(3)	12.813(2)	6.608(1)		1411.9(4)	LP
Al-MIL-53-NH_2-AS[43]	[Al(OH)(BDC-NH_2)]·0.3(H_2BDC-NH_2)	16.898(20)	12.539(18)	6.647(8)		1408.4(4)	LP
Al-MIL-53-NH_2-DMF[43]	[Al(OH)(BDC-NH_2)]·0.95(DMF)	17.578(17)	11.483(9)	6.630(6)		1338.9(25)	LP
Al-MIL-53-NH_2[43]	[Al(OH)(BDC-NH_2)]·0.9(H_2O)	19.722(7)	7.692(3)	6.578(4)	105.1(3)	961.5(10)	NP
Al-MIL-53-NHCHO-AS[43]	[Al(OH)(BDC-NHCHO)]·1.0(H_2O)	17.156(5)	12.246(5)	6.604(13)		1387.4(8)	LP
Al-MIL-53-$(COOH)_2$-AS[45]	[Al(OH)(BDC-$(COOH)_2$)]·0.1(H_2BDC-$(COOH)_2$))·1.5(H_2O)	17.54483(8)	13.57813(8)	6.66420(4)	113.1956(5)	1459.25(2)	LP

[a] Lattice parameters were determined from room temperature XRPD data, except the four high-temperature (HT) forms that were derived from the TDXRPD data. [b] LP: large-pore, NP: narrow-pore.

temperatures, the TG traces of the NP-forms of the compounds (Supporting Information, Figures S11−S15) display only one weight loss step owing to the removal of adsorbed water molecules. The observed weight losses of the NP-forms are consistent with the calculated ones as well as the elemental analyses (Supporting Information, Tables S1 and S2), indicating phase purity of the compounds. The removal of free water molecules from the channels occurs at about 100 °C for NP-forms of all the compounds. Evidently, the introduction of functional groups does not lead to a dramatic change of thermal stability or large activation barriers for the removal of H_2O molecules.

The high thermal stability of the Al-MIL-53-X compounds has also been verified by temperature-dependent XRPD (TDXRPD) measurements. From the TDXRPD patterns of the AS-form of **4-NO_2**- (Supporting Information, Figure S16), it becomes obvious that the compound is stable up to 380 °C. Since the AS-forms of the compounds do not switch to their high-temperature (HT) forms upon heating, they could not be activated by direct thermal treatment.

According to the TDXRPD patterns (Figures 2, 3 and Supporting Information, Figures S17−S19) recorded in capillary geometry, the NP-forms of **1-Cl**, **2-Br**, **3-CH_3**, **4-NO_2**, and **5-$(OH)_2$** are stable up to 525, 450, 500, 475, and 400 °C, respectively. The

dx.doi.org/10.1021/ic201219g |*Inorg. Chem.* 2011, 50, 9518–9526

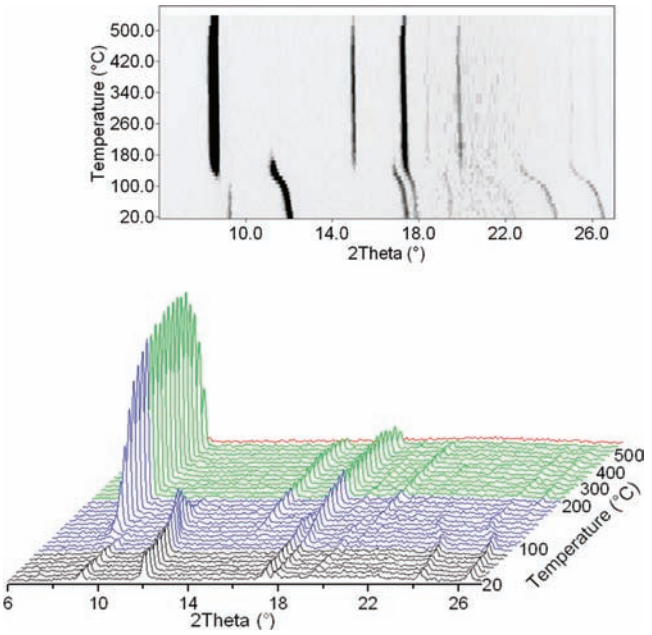

Figure 2. TDXRPD patterns of **1-Cl** under air atmosphere (Cu Kα radiation, λ = 1.5406 Å) in the range 20−550 °C. The top view of the patterns is shown on the top. Black patterns: NP-form; blue patterns: mixture of NP and HT-forms; green patterns: HT-form; red pattern: decomposed form.

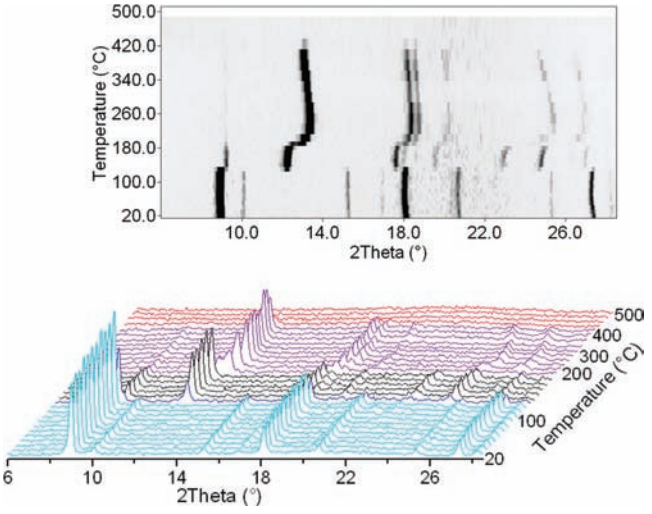

Figure 3. TDXRPD patterns of the water-rich form of **5-(OH)$_2$** under air atmosphere (CuKα radiation, λ = 1.5406 Å) in the range 20−500 °C. The top view of the patterns is shown on the top. Cyan patterns: water-rich (LP) form; black patterns: NP-form; violet patterns: NP-form with Bragg peaks shifted toward higher 2θ values; red patterns: decomposed form.

observation of higher decomposition temperatures during TDXRPD measurements compared to TGA can be assigned to the lower outer diameter (0.30 mm) of the thin-walled (thickness: 0.01 mm) capillaries which prevent sufficient air flow around the samples filled into them.

Breathing Behavior. On the basis of results of the unit cell determinations (Table 1), the structures of the different forms of Al-MIL-53-X were found to correspond to the ones observed in the nonfunctionalized[13] and amino-functionalized[43] Al-MIL-53. However, the modification of the pore environments with different functional groups results in different breathing behavior of the frameworks. The unit cell volumes of all the AS, guest-exchanged and HT-forms of the compounds vary in the ranges 1410−1457, 1352−1462, and 1420−1451 Å^3, respectively. Obviously, the AS, guest-exchanged and HT-forms of the compounds differ slightly from each other in terms of unit cell volumes, and all of these forms correspond to the LP-version of the frameworks. In sharp contrast, the unit cell volumes (955−1055 Å^3) of the hydrated compounds vary significantly from those of AS, guest-exchanged, and HT-forms, and thus the frameworks adopt the NP-forms. Conclusively, the breathing effect of the functionalized solids is dependent on both the nature of guest molecules and the temperature. Whereas some guest molecules (H_2BDC-X and DMF) allow the frameworks to exist in the LP-form, the others (H_2O) force them to adopt the NP-form.

To investigate the breathing properties of the Al-MIL-53-X compounds upon dehydration−rehydration, both temperature and time-dependent XRPD experiments were carried out on the NP-forms of the compounds. A typical TDXRPD analysis of the NP-form is illustrated in Figure 2 (here **1-Cl**, see Supporting Information, Figures S17−S19 for all the other compounds). The Bragg peaks of the NP-forms of all the compounds are exclusively observed below 80 °C. With increase in temperature, the Bragg reflections of the NP-forms gradually disappear, and new reflections of the HT-phases start to appear at different temperatures (**1-Cl**, 110 °C; **2-Br**, 80 °C; **3-CH$_3$**, 120 °C; **4-NO$_2$**, 130 °C) depending on the appended functional groups, as a consequence of both the departure of water and the thermal expansion.[57] The Bragg peaks of only the HT-forms are noticed in the following ranges: **1-Cl**, 210−525 °C; **2-Br**, 140−450 °C; **3-CH$_3$**, 325−500 °C; **4-NO$_2$**, 160−475 °C. The diffraction peaks of the HT-forms finally vanish above the range 400−525 °C, leading to the decomposition of the compounds into X-ray amorphous materials.

To examine the flexibility of the **5-(OH)$_2$** framework, a TDXRPD measurement was carried out on its water-rich (LP) form, that is, **5-(OH)$_2$-H$_2$O** (Figure 3). Therefore, **5-(OH)$_2$** was treated with an excess of water before the measurement. This leads to an uptake of water accompanied by the opening of the pores, which has been also observed in the unmodified Cr-MIL-53 material.[58] Below 120 °C, the LP-form is observed in the TDXRPD patterns. At 140 °C, the LP-form transforms completely into the NP-form which continues to exist up to 180 °C. In the range 190−400 °C, the positions of some of the Bragg reflections of the NP-form shift toward higher 2θ values. Slight shift of the positions of few of the diffraction peaks has also been observed in the TDXRPD patterns of the NP-form of Al-MIL-53-NH$_2$ (Supporting Information, Figure S20) in the range 120−450 °C. This alteration of the peak positions for both compounds can be attributed to the removal of water molecules from the pores. Evidently, the NP-forms of both compounds remains closed after heating.

A graphical summary of the results on the temperature-dependent breathing behavior of the different functionalized Al-MIL-53 compounds is given in the Supporting Information, Figure S21.

To determine the time needed for rehydration of the HT forms, the NP-forms of **1-Cl**, **2-Br**, **3-CH$_3$**, and **4-NO$_2$** were heated at 180 °C under vacuum for 2 h and subsequently the powder patterns in flat-plate geometry were collected at room temperature under air atmosphere. The mixtures of HT and NP-forms of **4-NO$_2$**, **1-Cl**, and **2-Br** (Supporting Information,

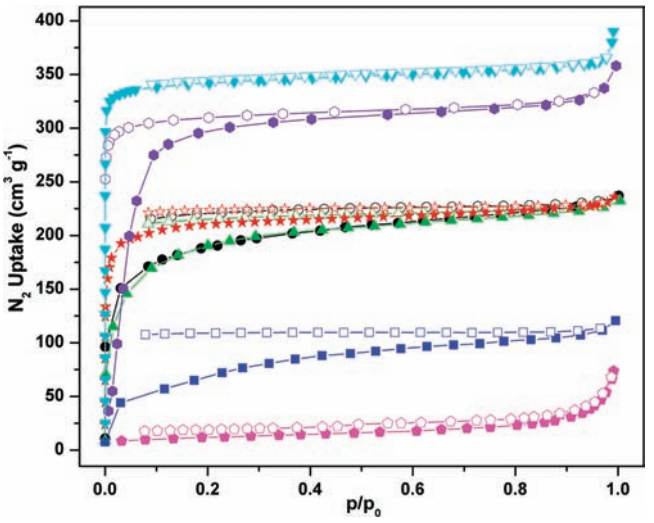

Figure 4. Low pressure N_2 adsorption (solid symbols) and desorption (empty symbols) isotherms of the thermally activated **1-Cl** (black, circles), **2-Br** (blue, squares), **3-CH_3** (green, triangles), **4-NO_2** (red, stars), **5-$(OH)_2$** (magenta, pentagons), Al-MIL-53-NH_2 (violet, hexagons), and Al-MIL-53 (cyan, upside-down triangles) measured at −196 °C.

Figures S21−S23) transform almost completely into their NP-forms after staying at room temperature for 0.15, 20, and 25 h, respectively. However, the transformation of a mixture of HT and NP-forms of **3-CH_3** (Supporting Information, Figure S24) into its NP-form remains incomplete, even after staying at ambient conditions for 23 h.

The introduction of different functionalities into the organic linkers of the frameworks thus influences the breathing phenomena of Al-MIL-53-X compounds. Notably, molecular mechanics simulations on the recently reported Fe-MIL-53-X compounds show that materials which easily convert from NP to LP-form (-CH_3, -$(CF_3)_2$) have free μ_2-OH groups, whereas the more energetically stable NP materials (-Cl, -Br, -NH_2, -$(OH)_2$) possess μ_2-OH groups that are involved in inorganic−organic intraframework H-bonds.[19] Therefore, a combination of guest-framework and intraframework H-bonding interactions effected by the attached functional groups may be attributed for the different breathing properties of the Al-MIL-53-X compounds. Compared to the here presented compounds, no significant breathing behavior during TDXRPD experiments was observed for the Fe-MIL-53-X compounds, which remain in their NP-forms in both dry and hydrated states, rendering the pores inaccessible to N_2.[19]

Sorption Properties. With the exception of **5-$(OH)_2$** the N_2 sorption measurements performed with the thermally activated Al-MIL-53-X compounds reveal type-I adsorption isotherms, but hysteresis is present for all functionalized compounds (Figure 4). The micropore volumes (Table 2) derived from the N_2 adsorption isotherms exhibit considerable porosities, which are lower than the one reported for nonfunctionalized Al-MIL-53.[13] Among the presented five compounds, **4-NO_2** adsorbs the highest amount of N_2. The N_2 accessible micropore volumes at a p/p_0 value of 0.9 decrease in the sequence: **4-NO_2** > **1-Cl** = **3-CH_3** > **2-Br** > **5-$(OH)_2$**. The lower N_2 uptake of **2-Br** compared to **1-Cl** and **3-CH_3** is probably due to the steric bulkiness of the −Br group compared to the −Cl and −CH_3

Table 2. Micropore Volumes[c] of the Al-MIL-53-X Solids Determined from N_2 and H_2O Adsorption Isotherms

compound	micropore volume (N_2; $cm^3\ g^{-1}$)	micropore volume (H_2O; $cm^3\ g^{-1}$)
1-Cl	0.32	0.14
2-Br	0.14	0.11
3-CH_3	0.32	0.11
4-NO_2	0.34	0.12
5-$(OH)_2$	0.07	0.42
Al-MIL-53	0.54	
Al-MIL-53-NH_2	0.44	0.10

[c] The micropore volumes of the Al-MIL-53-X compounds have been calculated at a p/p_0 value of 0.9.

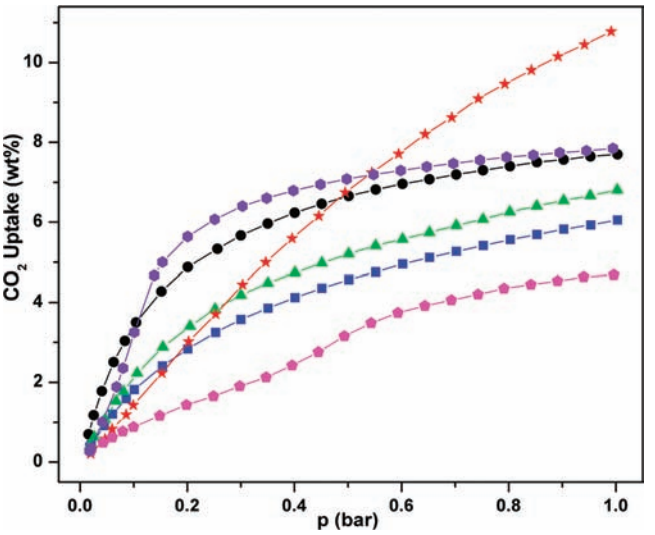

Figure 5. CO_2 adsorption isotherms of the thermally activated **1-Cl** (black, circles), **2-Br** (blue, squares), **3-CH_3** (green, triangles), **4-NO_2** (red, stars), **5-$(OH)_2$** (magenta, pentagons), and Al-MIL-53-NH_2 (violet, hexagons) measured at 25 °C.

functionalities. The inability of **5-$(OH)_2$** to show any N_2 uptake can be attributed to strong intraframework interactions [see TDXRPD patterns (Figure 3)]. Noticeably, **5-$(OH)_2$** has the smallest unit cell volume (Table 1) among the NP-forms of the five title compounds. The pores of the NP-form of **5-$(OH)_2$**, which are inaccessible to N_2, becomes clearly accessible to other gases having smaller kinetic diameters[59] and different adsorptive-framework interactions compared to N_2 (e.g., CO_2 and H_2O, Figures 5 and 6). Notably, the previously reported Al-MIL-53-NH_2 compound showed N_2 uptake higher than that of the presented five compounds.

The CO_2 adsorption properties of the thermally activated Al-MIL-53-X compounds were investigated at 25 °C up to 1 bar. As shown in Figure 5, the CO_2 adsorption isotherms of all compounds, except **5-$(OH)_2$**, follow type-I behavior in the pressure range from 0 to 1 bar. The deviation of the CO_2 adsorption isotherm of **5-$(OH)_2$** from type-I can be tentatively assigned to the breathing effect of its framework, which depends on the CO_2 pressure.

Adsorption isotherm of similar shape have been previously observed for parent M-MIL-53 (M = Al or Cr)[21−23] and Al-MIL-

dx.doi.org/10.1021/ic201219g |*Inorg. Chem.* 2011, 50, 9518–9526

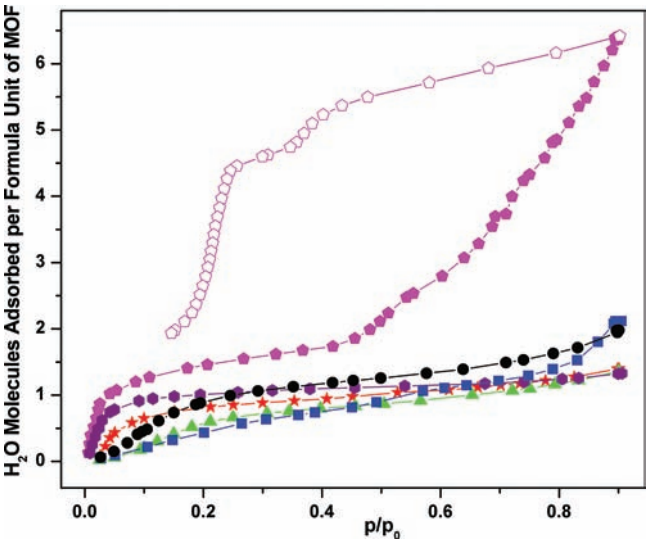

Figure 6. H_2O adsorption (solid symbols) and desorption (empty symbols) isotherms of the thermally activated **1-Cl** (black, circles), **2-Br** (blue, squares), **3-CH_3** (green, triangles), **4-NO_2** (red, stars), **5-$(OH)_2$** (magenta, pentagons), and Al-MIL-53-NH_2 (violet, hexagons) measured at 25 °C. The H_2O desorption isotherms for the thermally activated **1-Cl**, **2-Br**, **3-CH_3**, and **4-NO_2** (Supporting Information, Figure S25) are omitted for clarity.

53-NH_2[25,29] during high pressure CO_2 sorption studies. The descending order of CO_2 uptake values (wt %) at 1 bar is **4-NO_2** (10.8) > **1-Cl** (7.7) > **3-CH_3** (6.8) > **2-Br** (6.0) > **5-$(OH)_2$** (4.7). This CO_2 uptake sequence is in good agreement with the N_2 uptake trend of the compounds. In the pressure range 0.01−0.5 bar, Al-MIL-53-NH_2 captures the highest amount of CO_2 compared to the other compounds. This is due to the availability of CO_2 adsorption sites provided by the appended -NH_2 groups, as recently suggested by Stavitski et al.[28] and Torrisi et al.[60] based on computational studies. At 1 bar, the CO_2 uptake (7.85 wt %) of Al-MIL-53-NH_2, which has higher micropore volume than the presented compounds, exceeds that of **1-Cl**, **2-Br**, **3-CH_3**, and **5-$(OH)_2$**, but falls below that of **4-NO_2**. This fact can be attributed to the difficulty of opening the pores of Al-MIL-53-NH_2 at 1 bar and room temperature, which is in agreement with the temperature versus CO_2 pressure phase diagram of the compound derived by Denayer and co-workers.[29] Compared to unfunctionalized Al-MIL-53, the phase diagram of Al-MIL-53-NH_2 shows a larger stability domain of the NP form, which has been attributed to the increased affinity of the $-NH_2$ groups for CO_2. The computer simulations of Torrisi et al.[60] also claim that **5-$(OH)_2$** in its LP-form should adsorb the maximum amounts of CO_2 in the pressure range 0.01−0.5 bar, which is contrary to our observation. It should be noted that the simulations were performed on the LP-form of **5-$(OH)_2$**. However, both N_2 sorption and TDXRPD measurements show that the pores of **5-$(OH)_2$** are difficult to open probably because of several H-bonding interactions involving −OH functionalities. The fact that the NP-form of MIL-53 structure bearing BDC-$(OH)_2$ as a bridging ligand is energetically more stable than its LP-form has recently been predicted and in fact observed by Devic et al.[19] for Fe-MIL-53-$(OH)_2$ compound.

The H_2O adsorption−desorption properties (Figures 6 and Supporting Information, Figure S25) of the thermally activated Al-MIL-53-X compounds were examined at 25 °C. The H_2O accessible micropore volumes ($cm^3\ g^{-1}$) at a p/p_0 value of 0.9 decrease in the sequence: **5-$(OH)_2$** > **1-Cl** > **4-NO_2**> **2-Br** = **3-CH_3** (Table 2). This H_2O uptake trend is contrary to that observed during the N_2 and CO_2 sorption analyses of the compounds. The water-framework interactions (H-bonds) rather than availability of N_2 accessible micropore volume may be attributed for this trend. Whereas the less hydrophilic pore surfaces of **1-Cl**, **2-Br**, **3-CH_3**, **4-NO_2**, and Al-MIL-53-NH_2 show lower H_2O uptake (1−2 molecules per formula unit at p/p_0 = 0.9), the more hydrophilic pore surface of **5-$(OH)_2$** allows to capture six H_2O molecules per formula unit at p/p_0 = 0.9. The high H_2O uptake capacity of **5-$(OH)_2$** is consistent with the possibility of H-bonds between attached −OH groups and adsorbed water molecules. Upon adsorption of large amounts of H_2O, **5-$(OH)_2$** transforms from a NP-form (unit cell volume: 955 $Å^3$) into a water-rich (**5-$(OH)_2$-H_2O**) or LP-form (unit cell volume: 1365 $Å^3$) (Table 1). It is noteworthy that high water uptake comparable to that of **5-$(OH)_2$** has recently been reported by Devic et al. for Fe-MIL-53-$(OH)_2$ compound.[19]

The H_2O adsorption−desorption isotherms of **5-$(OH)_2$** display a wide hysteresis loop. The adsorption of H_2O on **5-$(OH)_2$** proceeds in two steps: after a very fast uptake (one H_2O molecule per formula unit) below the p/p_0 value of 0.1, the isotherm reaches its first plateau between the p/p_0 values 0.1 and 0.4, followed by an adsorption of five additional H_2O molecules per formula unit between the p/p_0 values 0.4 and 0.9. This type of unusual phenomenon has been previously observed during the high-pressure CO_2 sorption analysis of nonmodified M-MIL-53 (M = Al or Cr)[21−23] and Al-MIL-53-NH_2[25,29] can be interpreted based on the following hypothesis. After adsorption of the first portion of water, the degassed solid remains in NP-form similar to the hydrated material. At higher vapor pressures, the framework opens up and takes up additional H_2O molecules into the pores.

CONCLUSIONS

The synthesis, characterization, and structural analysis of five isoreticular functionalized flexible Al-MIL-53-X hybrid solids have been demonstrated. TGA and TDXRPD experiments carried out on the NP-form of the compounds show high thermal stability in the range 325−500 °C. Compared to the isotypic functionalized Fe-MIL-53-X solids,[19] most of the present compounds display significant microporosity toward N_2, CO_2, or H_2O. As expected from previous studies on the nonmodified parent Al-MIL-53,[13] all the functionalized frameworks retain their structural flexibility upon dehydration−rehydration. However, a complex combination of guest-framework and possible intraframework H-bonding interactions caused by the grafted functional groups leads to different breathing behavior. Finally, the study of the adsorption of various gases and water showed that the pore opening is selective and strongly depends on intraframework H-bonding and adsorptive-framework interactions, making these inexpensive, nontoxic, lightweight, and hydrolytically stable solids potential candidates for applications such as gas storage, catalysis, separations, drug delivery, and sensors, which can be envisaged from the larger accessibility of the pores in their open forms.

ASSOCIATED CONTENT

Supporting Information. XRPD patterns, IR spectra, TG curves, detailed H_2O sorption isotherms, tables containing TGA

dx.doi.org/10.1021/ic201219g |*Inorg. Chem.* 2011, 50, 9518–9526

results, elemental analysis, and IR frequencies. This material is available free of charge via the Internet at http://pubs.acs.org.

AUTHOR INFORMATION

Corresponding Author

*E-mail: stock@ac.uni-kiel.de. Phone: (+)49-4318801675. Fax: (+)49-4318801775.

ACKNOWLEDGMENT

The State of Schleswig-Holstein and the Deutsche Forschungsgemeinschaft (DFG, SPP 1362 "Porous Metal-Organic Frameworks" under the grant STO 643/5-1) are gratefully acknowledged for the financial support. We thank Dr. Thomas Devic (UVSQ, Versailles) for fruitful discussion concerning the results of the MIL-53-$(OH)_2$ data. The research leading to these results has received funding from the European Community's Seventh Framework Programme (FP7/2007-2013) under grant agreement no. 228862.

REFERENCES

(1) Férey, G. *Chem. Soc. Rev.* **2008**, *37*, 191.
(2) Kitagawa, S.; Kitaura, R.; Noro, S. *Angew. Chem., Int. Ed.* **2004**, *43*, 2334.
(3) Yaghi, O. M.; O'Keeffe, M.; Ockwig, N. W.; Chae, H. K.; Eddaoudi, M.; Kim, J. *Nature* **2003**, *423*, 705.
(4) Lee, J.; Farha, O. K.; Roberts, J.; Scheidt, K. A.; Nguyen, S. T.; Hupp, J. T. *Chem. Soc. Rev.* **2009**, *38*, 1450.
(5) Ma, L.; Abney, C.; Lin, W. *Chem. Soc. Rev.* **2009**, *38*, 1248.
(6) Murray, L. J.; Dinca, M.; Long, J. R. *Chem. Soc. Rev.* **2009**, *38*, 1294.
(7) Li, J.-R.; Kuppler, R. J.; Zhou, H.-C. *Chem. Soc. Rev.* **2009**, *38*, 1477.
(8) Hamon, L.; Llewellyn, P. L.; Devic, T.; Ghoufi, A.; Clet, G.; Guillerm, V.; Pirngruber, G. D.; Maurin, G.; Serre, C.; Driver, G.; van Beek, W.; Jolimaitre, E.; Vimont, A.; Daturi, M.; Férey, G. *J. Am. Chem. Soc.* **2009**, *131*, 17490.
(9) Taylor-Pashow, K. M. L.; Della Rocca, J.; Xie, Z. G.; Tran, S.; Lin, W. B. *J. Am. Chem. Soc.* **2009**, *131*, 14261.
(10) Horcajada, P.; Chalati, T.; Serre, C.; Gillet, B.; Sebrie, C.; Baati, T.; Eubank, J. F.; Heurtaux, D.; Clayette, P.; Kreuz, C.; Chang, J. S.; Hwang, Y. K.; Marsaud, V.; Bories, Y.-N.; Cynober, L.; Gil, S.; Férey, G.; Couvreur, P.; Gref, R. *Nat. Mater.* **2010**, *9*, 172.
(11) Serre, C.; Millange, F.; Thouvenot, C.; Nogues, M.; Marsolier, G.; Louer, D.; Ferey, G. *J. Am. Chem. Soc.* **2002**, *124*, 13519.
(12) Whitfield, T. R.; Wang, X.; Liu, L.; Jacobson, A. J. *Solid State Sci.* **2005**, *7*, 1096.
(13) Loiseau, T.; Serre, C.; Huguenard, C.; Fink, G.; Taulelle, F.; Henry, M.; Bataille, T.; Férey, G. *Chem.—Eur. J.* **2004**, *10*, 1373.
(14) Vougo-Zanda, M.; Huang, J.; Anokhina, E.; Wang, X.; Jacobson, A. J. *Inorg. Chem.* **2008**, *47*, 11535.
(15) Anokhina, E. V.; Vougo-Zanda, M.; Wang, X.; Jacobson, A. J. *J. Am. Chem. Soc.* **2005**, *127*, 15000.
(16) Férey, G.; Serre, C. *Chem. Soc. Rev.* **2009**, *38*, 1380.
(17) Millange, F.; Guillou, N.; Walton, R. I.; Grenèche, J. M.; Margiolaki, I.; Férey, G. *Chem. Commun.* **2008**, 4732.
(18) Volkringer, C.; Loiseau, T.; Guillou, N.; Férey, G.; Elkaïm, E.; Vimont, A. *Dalton Trans.* **2009**, 2241.
(19) Devic, T.; Horcajada, P.; Serre, C.; Salles, F.; Maurin, G.; Moulin, B.; Heurtaux, D.; Clet, G.; Vimont, A.; Grenèche, J.-M.; Le Ouay, B.; Moreau; Magnier, E.; Filinchuk, Y.; Marrot, J.; Lavalley, J.-C.; Daturi, M.; Férey, G. *J. Am. Chem. Soc.* **2010**, *132*, 1127.
(20) Millange, F.; Serre, C.; Guillou, N.; Férey, G.; Walton, R. I. *Angew. Chem., Int. Ed.* **2008**, *47*, 4100.
(21) Serre, C.; Bourrelly, S.; Vimont, A.; Ramsahye, N. A.; Maurin, G.; Llewellyn, P. L.; Daturi, M.; Filinchuk, Y.; Leynaud, O.; Barnes, P.; Férey, G. *Adv. Mater.* **2007**, *19*, 2246.
(22) Bourrelly, S.; Llewellyn, P. L.; Serre, C.; Millange, F.; Loiseau, T.; Férey, G. *J. Am. Chem. Soc.* **2005**, *127*, 13519.
(23) Boutin, A.; Coudert, F.-X.; Springuel-Huet, M.-A.; Neimark, A. V.; Férey, G.; Fuchs, A.-H. *J. Phys. Chem. C* **2010**, *114*, 22237.
(24) Boutin, A.; Couck, S.; Coudert, F.-X.; Serra-Crespo, P.; Gascon, J.; Kapteijn, F.; Fuchs, A. H.; Denayer, J. F. M. *Microporous Mesoporous Mater.* **2011**, *140*, 108.
(25) Couck, S.; Denayer, J. F. M.; Baron, G. V.; Rémy, T.; Gascon, J.; Kapteijn, F. *J. Am. Chem. Soc.* **2009**, *131*, 6326.
(26) V. Finsy, V.; Maa, L.; Alaerts, L.; De Vos, D. E.; Baron, G. V.; Denayer, J. F. M. *Microporous Mesoporous Mater.* **2009**, *120*, 221.
(27) Salles, F.; Ghoufi, A.; Maurin, G.; Bell, R. G.; Mellot-Draznieks, C.; Férey, G. *Angew. Chem., Int. Ed.* **2008**, *47*, 8487.
(28) Stavitski, E.; Pidko, E. A.; Couck, S.; Remy, T.; Hensen, E. J. M.; Weckhuysen, B. M.; Denayer, J.; Gascon, J.; Kapteijn, F. *Langmuir* **2011**, *27*, 3970.
(29) Boutin, A.; Couck, S.; Coudert, F.-X.; Serra-Crespo, P.; Gascon, J.; Kapteijn, F.; Fuchs, A. H.; Denayer, J. F. M. *Microporous Mesoporous Mater.* **2011**, *140*, 108.
(30) Llewellyn, P. L.; Maurin, G.; Devic, T.; Loera-Serna, S.; Rosenbach, N.; Serre, C.; Bourrelly, S.; Horcajada, P.; Filinchuk, Y.; Férey, G. *J. Am. Chem. Soc.* **2008**, *130*, 12808.
(31) Couck, S.; Rémy, T.; Baron, G. V.; Gascon, J.; Kapteijn, F.; Denayer, J. F. M. *Phys. Chem. Chem. Phys.* **2010**, *12*, 9413.
(32) Llewellyn, P. L.; Horcajada, P.; Maurin, G.; Devic, T.; Rosenbach, N.; Bourrelly, S.; Serre, C.; Vincent, D.; Loera-Serna, S.; Filinchuk, Y.; Férey, G. *J. Am. Chem. Soc.* **2009**, *131*, 13002.
(33) Trung, T. K.; Trens, P.; Tanchoux, N.; Bourrelly, S.; Llewellyn, P. L.; Loera-Serna, S.; Serre, C.; Loiseau, T.; Fajula, F.; Férey, G. *J. Am. Chem. Soc.* **2008**, *130*, 16926.
(34) Alaerts, L.; Maes, M.; Giebeler, L.; Jacobs, P. A.; Martens, J. A.; Denayer, J. F. M.; Kirschhock, C. E. A.; De Vos, D. E. *J. Am. Chem. Soc.* **2008**, *130*, 14170.
(35) Finsy, V.; Kirschhock, C. E. A.; Vedts, G.; Maes, M.; Alaerts, L.; De Vos, D. E.; Baron, G. V.; Denayer, J. F. M. *Chem.—Eur. J.* **2009**, *15*, 7724.
(36) Bauer, S.; Serre, C.; Devic, T.; Horcajada, P.; Marrot, J.; Férey, G.; Stock, N. *Inorg. Chem.* **2008**, *47*, 7568.
(37) Sanselme, M.; Grenèche, J.-M.; Riou-Cavellec, M.; Férey, G. *Solid State Sci.* **2004**, *6*, 853.
(38) Volkringer, C.; Popov, D.; Loiseau, T.; Férey, G.; Burghammer, M.; Riekel, C.; Haouas, M.; Taulelle, F. *Chem. Mater.* **2009**, *21*, 5695.
(39) Loiseau, T.; Lecroq, L.; Volkringer, C.; Marrot, J.; Férey, G.; Haouas, M.; Taulelle, F.; Bourrelly, S.; Llewellyn, P. L.; Latroche, M. *J. Am. Chem. Soc.* **2006**, *128*, 10223.
(40) Volkringer, C.; Popov, D.; Loiseau, T.; Guillou, N.; Férey, G.; Haouas, M.; Taulelle, F.; Mellot-Draznieks, C.; Burghammer, M.; Riekel, C. *Nat. Mater.* **2007**, *6*, 760.
(41) Gascon, J.; Aktay, U.; Hernandez-Alonso, M. D.; van Klink, G. P. M.; Kaptejin, F. *J. Catal.* **2009**, *261*, 75.
(42) Stavitski, E.; Pidko, E. A.; Couck, S.; Remy, T.; Hensen, E. J. M.; Weckhuysen, B. M.; Denayer, J.; Gascon, J.; Kapteijn, F. *Langmuir* **2011**, *27*, 3970.
(43) Ahnfeldt, T.; Gunzelmann, D.; Loiseau, T.; Hirsemann, D.; Senker, J.; Férey, G.; Stock, N. *Inorg. Chem.* **2009**, *48*, 3057.
(44) Himsl, D.; Wallacher, D.; Hartmann, M. *Angew. Chem., Int. Ed.* **2009**, *48*, 4639.
(45) Volkringer, C.; Loiseau, T.; Guillou, N.; Férey, G.; Haouas, M.; Taulelle, F.; Elkaim, E.; Stock, N. *Inorg. Chem.* **2010**, *49*, 9852.
(46) Comotti, A.; Bracco, S.; Sozzani, P.; Horike, S.; Matsuda, R.; Chen, J.; Takata, M.; Kubota, Y.; Kitagawa, S. *J. Am. Chem. Soc.* **2008**, *130*, 13664.
(47) Garibay, S. J.; Wang, Z.; Cohen, S. M. *Inorg. Chem.* **2010**, *49*, 8086.
(48) Volkringer, C.; Cohen, S. M. *Angew. Chem., Int. Ed.* **2010**, *49*, 4644.

(49) Nguyen, J. G.; Cohen, S. M. *J. Am. Chem. Soc.* **2010**, *132*, 4560.
(50) Meilikhov, M.; Yusenko, K.; Fischer, R. A. *J. Am. Chem. Soc.* **2009**, *131*, 9644.
(51) Meilikhov, M.; Yusenko, K.; Fischer, R. A. *Dalton Trans.* **2010**, *39*, 10990.
(52) Meilikhov, M.; Yusenko, K.; Fischer, R. A. *Dalton Trans.* **2009**, 600.
(53) Boultif, A.; Louer, D. *J. Appl. Crystallogr.* **1991**, *24*, 987.
(54) *STOE WinXPOW*, version 2.11; Stoe & Cie GmbH: Darmstadt, Germany, 2005.
(55) Banwell, C. N.; McCash, E. M. *Fundamentals of Molecular Spectroscopy*; McGraw Hill: New York, 1994.
(56) Costentin, C.; Robert, M.; Saveant, J. M. *J. Am. Chem. Soc.* **2006**, *128*, 8726.
(57) Barthelet, K.; Marrot, J.; Riou, D.; Férey, G. *Angew. Chem., Int. Ed.* **2002**, *41*, 281.
(58) Guillou, N.; Millange, F.; Walton, R. I. *Chem. Commun.* **2011**, *47*, 713.
(59) Li, J.-R.; Kuppler, R. J.; Zhou, H. C. *Chem. Soc. Rev.* **2009**, *38*, 1477.
(60) Torrisi, A.; Bell, R. G.; Mellot-Draznieks, C. *Cryst. Growth Des.* **2010**, *10*, 2839.